Polystyrene/Polybutadiene Blends: An Analysis of the Phase-Inversion Region and Cophase Continuity and a Comparison with Theoretical Predictions

Susan Joseph,[1] Maria Rutkowska,[2] Mariola Jastrzêbska,[2] Helena Janik,[3] Jozef T. Haponiuk,[3] Sabu Thomas[4]

[1]*Stephen's College, Pathanapuram, Kerala, India, 689695*
[2]*Gdynia Maritime Academy, 83 Morska Street, 81-225, Gdynia, Poland*
[3]*Polymer Tech Department, Chemical Faculty, Technical University of Gdansk, 80-952, Gdansk, Poland*
[4]*School of Chemical Sciences, Mahatma Gandhi University, Priyadarshini Hills P.O., Kottayam, Kerala, India, 686560*

Received 26 April 2002; accepted 23 October 2002

ABSTRACT: Blends of polystyrene and polybutadiene were prepared by melt mixing. The melt rheology behavior of the blends was studied with a capillary rheometer. The morphology of the blends was examined with scanning electron microscopy. The levels of continuity and cocontinuity were studied by both morphology and dissolution techniques. The region of phase inversion was observed at 50 wt % polystyrene. Various theoretical models were applied to determine the region of cophase continuity and to locate the point of phase inversion. © 2003 Wiley Periodicals, Inc. J Appl Polym Sci 89: 1007–1016, 2003

Key words: polymer blends; phase in version; polystyrene

INTRODUCTION

The melt blending of polymers is one of the cheapest and most cost-effective routes of tailoring materials for specific applications. Thermoplastic elastomers prepared from rubber–plastic blends are materials that combine the excellent processability characteristics of plastics at high temperatures and the wide range of physical properties of elastomers at service temperatures. These materials have gained great importance in recent years because of their many end-use applications.[1]

Compatibility is a desirable property in industrial fields for ease of fabrication and resistance to gross phase segregation during the cooling process of molten mixtures in product manufacturing. However, most polymer blends are immiscible and lead to heterogeneous morphology on blending. The type of morphology and its phase dimensions determine the blend properties. There are several methods for compatibilizing an immiscible pair, among which the generation of a cocontinuous morphology is of prime importance. By adjustments to the viscosity and composition, a cocontinuous morphology can be generated for a maximum interfacial contact area. In a cocontinuous morphology, each of the blend components takes its part directly in the load sharing process without the transfer of stress across the interphase. However, this technique may not be feasible for blends with very different homopolymer viscosities.

An important aspect of phase morphology is the microstructure, that is, the size, shape, and distribution of dispersed particles or the coarseness and tortuosity of a continuous phase. Polyblend morphology is understood as the mostly qualitative description of the spatial arrangement of blend component phases. Three basic morphologies are those of dispersed, stratified, and cocontinuous phases. During melt blending, the minor phase is broken up to form the dispersed phase. The interfacial tension, rheological properties, volume fractions of the components, melt viscosity, and complex strain field in the mixer (temperature, time, intensity of mixing, nature of flow, etc.) control both the size and shape of the dispersed phase. One of the key factors for achieving desired properties is control over the morphology type and dimensions. Droplet–matrix morphologies improve the impact properties,[2] fibrillar morphologies result in better tensile properties,[3,4] blends with a lamellar structure enhance barrier properties,[5,6] and cocontinuous morphologies show a combination of the characteristics of both polymer components. Willemse et al.[7] reported an increase in modulus from 400 to 750 MPa in a blend of 30% polystyrene (PS) in polyethylene with a change from a droplet–matrix structure to a fully cocontinuous structure; this indicates that cocontinuous morphologies are a versatile means of obtaining new polymeric materials. Both continuous and cocontinuous

Correspondence to: S. Thomas (sabut552001@yahoo.com).
Contract grant sponsor: International Division of the Department of Science and Technology (Delhi, India).
Contract grant sponsor: KBN (Poland).

morphologies can be generated for polymer blends, but the mechanism controlling them is still vague. However, for applications including barrier properties and polymer conductivity, the mechanism controlling the morphology[8] is essential. Several articles have appeared concerning the morphology of the dispersed phase. Relatively little is known about the composition range and processing conditions at which cocontinuity can be formed. Arns et al.[9] wrote a pioneering work concerning the influence of morphology on various macroscopic properties, helping to provide a framework within which the properties of polymer blends could be predicted and controlled. Lee and Han[10] performed an extensive study on PS/poly(methyl methacrylate) systems to investigate the stability of cocontinuous morphologies.

The usual technique used to investigate the morphologies of immiscible polymer blends is scanning electron microscopy (SEM), which is applied to the surfaces of cryofractures. However, this technique gives a picture of only a minute portion of the sample. Moreover, from a two-dimensional picture, it is not easy to estimate when phase inversion occurs as a function of composition and when the level of phase cocontinuity, a typical three-dimensional property, reaches a maximum. Additional solubility tests have been performed so that we could assess the region of phase inversion. We have used a solvent dissolution technique to complement the information provided by SEM. This technique is highly dependent on the morphology of polymer blends as long as the individual constituents exhibit different physical properties. However, the selective extraction technique of removing the minor constituent from immiscible polymer blends should be used with caution only as a method of quantifying the continuity because the extraction process can induce physical damage to the insoluble phase.

Continuity and phase inversion

The development of a cocontinuous morphology in polymer blends is one of the most interesting but least understood phenomena because of its complexity and a lack of characterization methods. The continuity of phases has a great impact on the resultant macroscopic properties of blends. According to Veenstra et al.,[11] cocontinuous morphologies are formed not in a single volume fraction but rather over a wide range of volume fractions; the range of the volume fractions depends on the processing conditions and the rheological properties of the blend components. Percolation theory deals with the development of continuity polymer blends. According to this theory, at low concentrations, there is a dispersion of particles in the matrix. A gradual change in the structure, from dispersed to fully cocontinuous, takes place in heterogeneous polymer blends with an increasing volume fraction of the minor component.[12] In dilute systems, droplet–matrix structures prevail. At higher volume fractions, starting at the percolation threshold, interconnected structures of the minor component develop until, at still higher volume fractions, the entire minor component is incorporated into a single continuous phase network inside the matrix component and a fully cocontinuous morphology is obtained. This continuous morphology can exist over a range of compositions, depending on the blending conditions.[2] Beyond this range, at still higher volume fractions, the phase network of the erstwhile matrix component starts breaking down until finally this component becomes dispersed. This is because, as the concentration of the minor phase increases, particles become close enough to behave as if they were connected. The further addition of minor-phase material extends the continuity network until the minor phase is continuous throughout the sample. It has generally been observed that a dispersed morphology is formed when the blend composition is highly asymmetric; a cocontinuous morphology is formed when the minor component, having higher melt viscosity, forms the discrete phase (the droplets), and the major component, having lower melt viscosity, forms the continuous phase.

Phase inversion is an adaptation of the system to an increase in the fraction of the minor phase. At a certain composition, both immiscible phases are completely continuous (100% continuous), and there is no possible distinction between the matrix and the dispersed phase. Phase inversion and dual-phase continuity can be used interchangeably. Knowledge of the dual-phase threshold may help in the design of blended materials. The percolation threshold is particularly important in the design of conducting polymer composite materials. The percolation of a continuous conducting phase in an insulating matrix is required to achieve conductivity throughout the sample.

In this work, the phase morphology of PS/polybutadiene (PB) blends was studied as a function of the blend composition, and fundamental investigations were made into the location of cocontinuity and the point of phase inversion. A combination of SEM and extraction experiments was used in determining whether the blend was cocontinuous or not. The phase morphology of melt-mixed samples and extraction experiments were studied with SEM. Various theoretical models were applied to find the region of cophase continuity and to locate the point of phase inversion.

TABLE I
Characteristics of the Materials

Material	Density (g cm^{-3})	Weight-average molecular weight
PS (atactic)	1.04	3.51×10^5
PB	0.94	5.3×10^5

EXPERIMENTAL

Materials

PS (crystal-grade; Polystron 678 SF-1), supplied by Polychem Limited (India), and cis-1,4-polybutadiene, supplied by Indian Petrochemical Co., Ltd. (Vadodara, India) under the trade name Cisamer G.P., were used in this work. The characteristics of the materials are given in Table I.

Preparation of the blends

The blends of PS and PB were prepared with a Haake Rheocord mixer. One of the blend components, PS, was premixed for 2 min to turn it into a melt, and the second component, PB, was introduced into the melt in bits. The mixing was recorded from the moment at which all the PB had been introduced. The temperature, rotor speed, and mixing time were 180°C, 60 rpm, and 8 min, respectively. The melt-mixed samples were denoted S_{00}, S_{10}, S_{20}, S_{30}, S_{40}, S_{50}, S_{60}, S_{70}, S_{80}, and S_{100}, where S represents PS and the subscripts indicate the contents of PS in the blends.

Characterization

Rheological measurements

A Gottfert capillary rheometer (Gottfert Werkstooff-Prufmaschinein GmbH) with a length/diameter ratio of 30 was used to measure the melt viscosity of the polymers as a function of the shear rate at an angle of entry of 180°. The measurements were made at 180°C. The shear rate changes from 5 to 300 s^{-1} were investigated.

Morphology analysis

Both the extracted and melt-mixed blend samples were cryofractured to yield brittle fractures; this avoided large deformations in the surfaces to be examined by SEM. The fracture surfaces were coated with a thin layer of gold. After the gold coating, the morphology was examined with a Philips XL20 model scanning electron microscope (Philips City, Netherlands). The scanning electron microscope was operated with secondary electrons at 20 kV. Fracture surfaces are normally very rough for cocontinuous blends.

The morphology studies were quantified by the counting of over 400 particles from several fields of view. The sizes of the dispersed domains measured from different micrographs were quantified in terms of different domain diameters.[12] These include the number-average domain diameter ($\bar{D}_n$), weight-average domain diameter ($\bar{D}_w$), surface-average domain diameter ($\bar{D}_s$), area-average domain diameter, and volume-average domain diameter ($\bar{D}_v$):

$$\bar{D}_n = \frac{\sum N_i D_i}{\sum N_i} \tag{1}$$

$$\bar{D}_w = \frac{\sum N_i D_i^2}{\sum N_i D_i} \tag{2}$$

$$\bar{D}_s = \sqrt{\frac{\sum N_i D_i^2}{N_i}} \tag{3}$$

$$\bar{D}_v = \frac{\sum N_i D_i^4}{\sum N_i D_i^3} \tag{4}$$

In these equations, N_i is the number of domains with diameter D_i. The polydispersity index (PDI), a measure of the domain size distribution, was also calculated with the following relation:

$$\text{PDI} = \frac{\bar{D}_w}{\bar{D}_n} \tag{5}$$

Cocontinuity calculation/solvent dissolution

The cocontinuity in the blend was checked with dissolution experiments.[13] The solvents were carefully chosen for the complete dissolution of one of the components without the other component being affected. Melt-mixed samples of a uniform length were weighed and fully immersed in an etchant at room temperature for 5 days. This was sufficient for the complete removal of the soluble fraction. Each polymer blend concentration was dissolved in separate bottles. The PS phase was extracted from the blends with butan-2-one, and the PB phase was extracted with *n*-heptane. Then, the remains were taken out of the solvent, dried at 70°C, and weighed carefully. For blends consisting of a matrix with dispersed particles, etching of the matrix caused a complete disintegration of the blend material, and a milky suspension was obtained. A blend was only considered fully cocontinuous if 100% of one component could be extracted and the remaining piece was still self-supporting. The percentage of continuity was defined as the weight ratio of the minor

phase involved in a continuous path divided by the total weight of the minor phase:

$$\text{Continuity index} = \frac{\text{Weight of the initial component} - \text{Weight after extraction}}{\text{Initial weight of the component}} \quad (6)$$

Experimental morphology changes in the blend

Besides SEM scanning electron microscope, Bu and He[14] used a method of macroscopic characterization for determining the continuous or dispersed state of each phase. They reported the phase morphology by SEM observations in an A/B blend by dissolution tests after dissolving B. The method consisted of macroscopic observations (by the naked eye) of sample shapes and a comparison of the weight percentage of the remaining phase A after the extraction of B. Here W_0 is the original weight of phase A in the blend, and W_r is the weight percentage of the remaining phase A after the extraction of B. According to Bu and He, if there is no change in shape and W_r is greater than W_0, phase A is continuous, and phase B is dispersed or partly continuous. Also, if there is no change on dissolution and W_r is equal to W_0, A and B are continuous. If W_r is less than W_0, phase A is mostly continuous, and phase B is continuous.

Cocontinuity models

In the literature, several empirical relations were proposed to describe the point of phase inversion. Jordhamo et al.[15] proposed the following expression, which is based on the viscosity ratio and volume fractions, to predict the location of the point of phase inversion or cophase continuity in immiscible polymer blends. Generally, the phase with the larger volume fraction tends to be the continuous phase. The phase with the lower viscosity also tends to be continuous because of its tendency to flow around the higher viscosity phase:

$$\frac{\eta_1\phi_2}{\eta_2\phi_1} = 1 \quad (7)$$

In this equation, η_1 and η_2 denote the melt viscosities (Pa s), and ϕ_1 and ϕ_2 are the volume fractions of the pure components of the binary blend. If ϕ_1/ϕ_2 is higher than η_1/η_2, phase 1 is continuous and reciprocal; phase 2 is continuous if ϕ_1/ϕ_2 is lower than η_1/η_2. Jordhamo et al.'s model, however, is limited to low shear rates and does not consider the variations in interfacial tension between the phases.

Chen and Su[16] proposed another model, considering the fact that the Jordhamo model overestimates the volume fraction of the high-viscosity phase. This model is limited to low shear rates and does not consider the effect of variations in interfacial tension. According to this model,

$$\frac{\phi h\nu}{\phi l\nu} = 1.2\left(\frac{\eta h\nu}{\eta l\nu}\right)^{0.3} \quad (8)$$

where $h\nu$ and $l\nu$ indicate high- and low-viscosity phases, respectively. Chen and Su again modified this model and proposed another model by deleting 1.2 from the previous equation:[17]

$$\frac{\phi h\nu}{\phi l\nu} = \left(\frac{\eta h\nu}{\eta l\nu}\right)^{0.3} \quad (9)$$

The model proposed by Paul and Barlow[18] is based on observations made by Avgeropoulos et al.:[19]

$$\frac{\phi_1}{\phi_2} = \frac{\eta_1(\dot\gamma)}{\eta_2(\dot\gamma)} \quad (10)$$

where ϕ_x is the volume fraction of x at phase inversion and η_x is the viscosity of phase x. This model has been corroborated,[20] but exceptions have also been reported.[21,22] The model according to Metlkin and Blekht[8] gives the following relation:

$$\phi_1 = \left[1 + \frac{\eta_1}{\eta_2}\left(1 + 2.25\log\left(\frac{\eta_1}{\eta_2}\right) + 1.81\left(\log\left(\frac{\eta_1}{\eta_2}\right)\right)^2\right)\right]^{-1} \quad (11)$$

We have applied the aforementioned models to locating the region of phase inversion theoretically. Utracki[23] developed a better expression for predicting phase inversion based on emulsion theory:

$$\frac{\eta_1}{\eta_2} = \left(\frac{\phi_m - \phi_2}{\phi_m - \phi_1}\right)(\eta)\phi_m \quad (12)$$

where ϕ_m refers to the volume fraction of the matrix at the percolation point and (η) refers to the intrinsic viscosity of the dispersed phase. All these models predict that the less viscous phase will have the greatest tendency to be the continuous phase.

As previously mentioned, all these models developed to predict the phase-inversion point only consider the viscosity ratio. It is possible, however, that elasticity also plays an important role.[15] Van Oene[24] developed an expression to describe an elastic contribution to the interfacial tension under dynamic conditions:

$$\nu_{\text{eff}} = \nu + d/12[(N_2)_d - (N_2)_m] \quad (13)$$

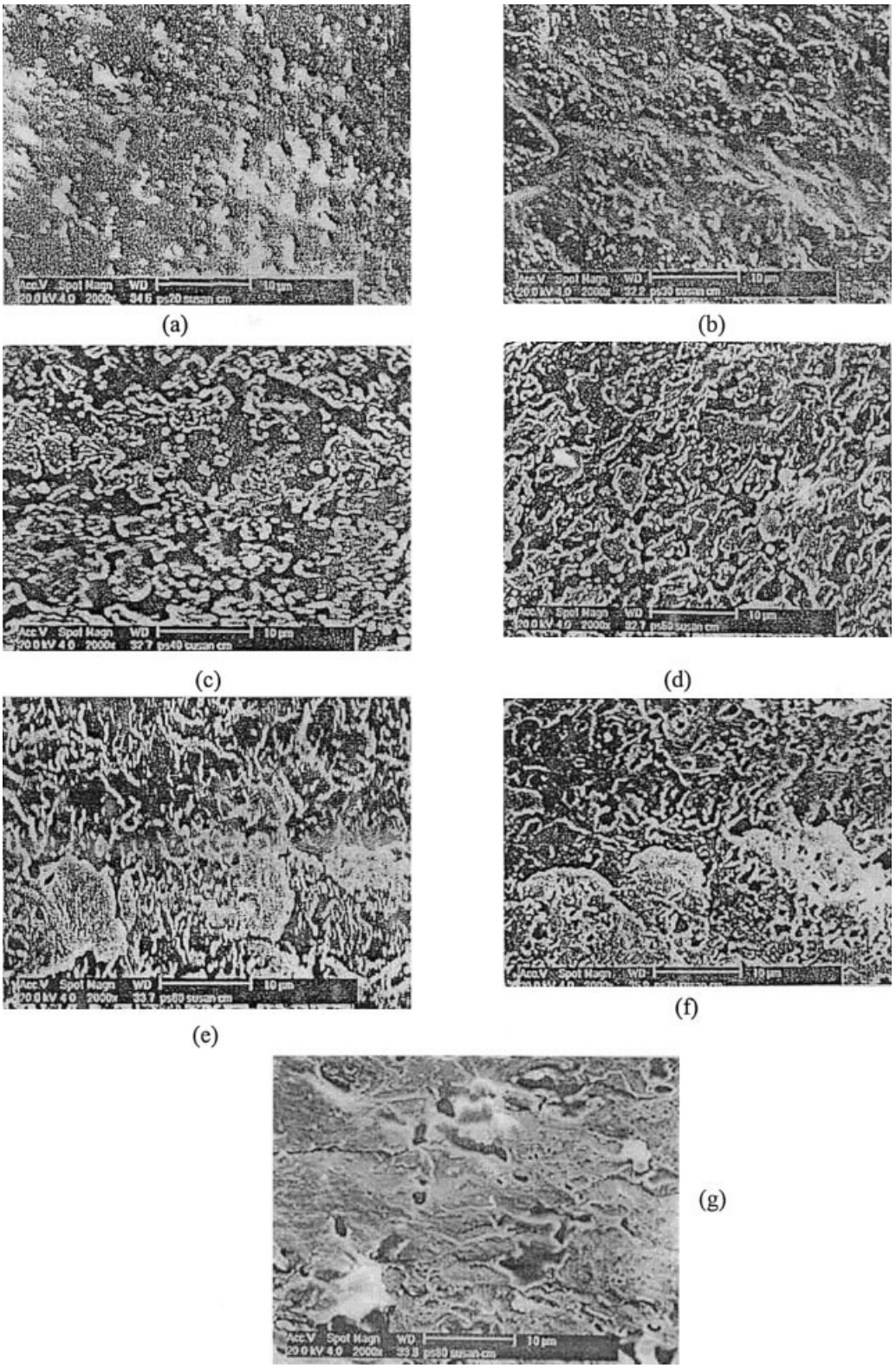

Figure 1 SEM micrographs of unextracted binary PS/PB blends: (a) 20/80, (b) 30/70, (c) 40/60, (d) 50/50, (e) 60/40, (f) 70/30, and (g) 80/20.

where ν_{eff} is the effective interfacial tension, ν is the interfacial tension, d is the droplet diameter, N_d is the second normal stress function (dispersed phase), and, N_m is the second normal stress function (matrix).

In this study, we made an attempt to determine the region of dual-phase continuity and the onset of percolation for PS/PB blends prepared by melt mixing by a combination of macroscopic, microscopic, and sol-

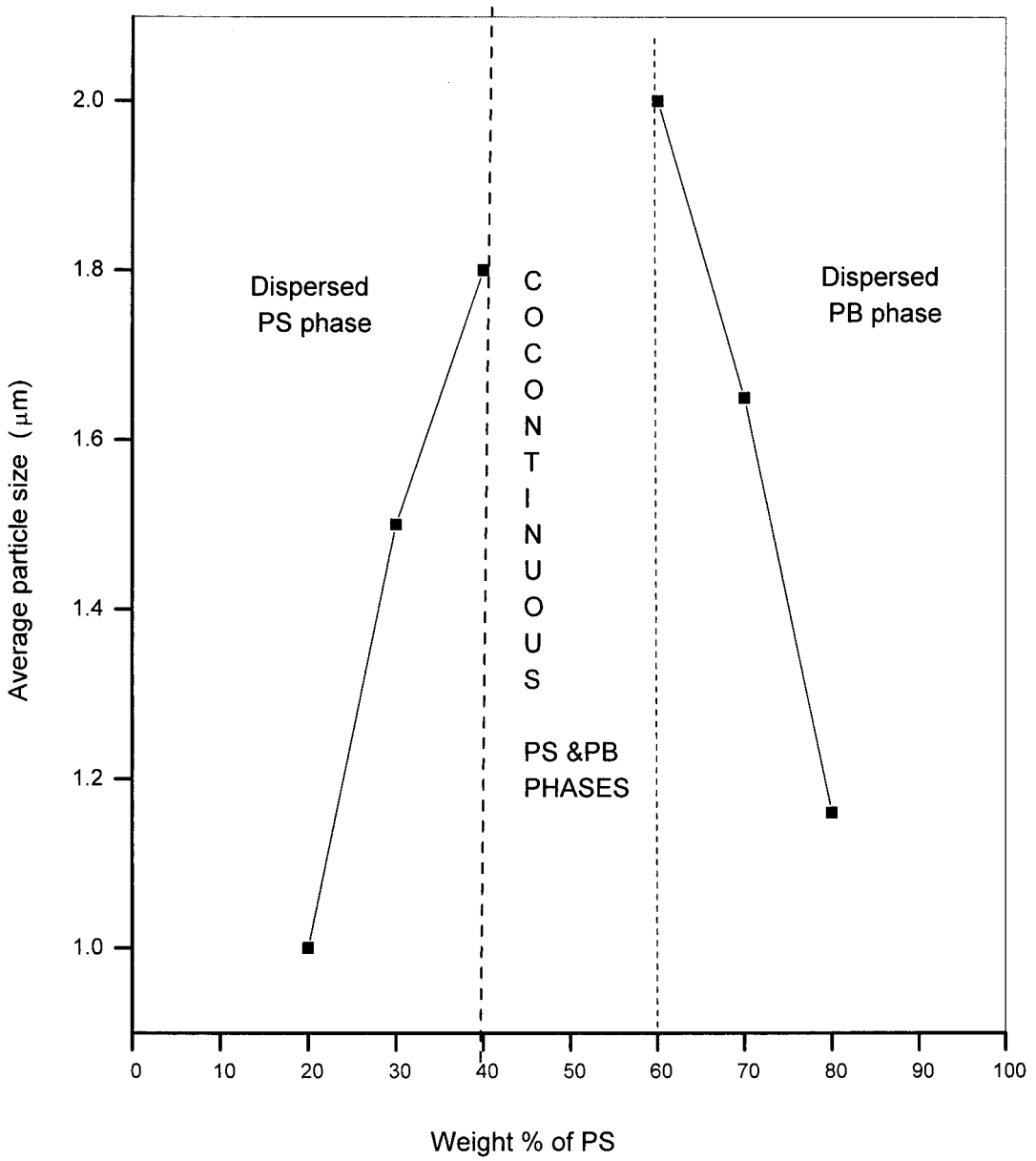

Figure 2 Effect of the blend composition on the dispersed particle size.

vent dissolution techniques. Various theoretical models were applied to estimate the location of phase inversion.

RESULTS AND DISCUSSION

Morphological observations

There are reports that dispersive forces in immiscible blends are deformable and may give rise to a wide range of sizes and shapes during processing, which, in turn, determine the morphology of the system. The phase morphology of an immiscible blend changes with the composition, from a dispersion system to an inverse dispersion system, through phase inversion[19] (dual-phase continuity). SEM micrographs of unextracted binary PS/PB blends are given in Figure 1(a–g). The micrographs demonstrate a two-phase morphology. At low enough concentrations of the dispersed phase, there is only drop breakup, as seen for S_{20} in Figure 1(a). The morphology of S_{30} shows that at high PB contents, the minor phase of PS is dispersed as spherical inclusions in the continuous PB matrix, as seen in Figure 1(b). For the S_{40} blend in Figure 1(c), both dispersed and continuous phases are seen. When PS is the dispersed phase, the rate of coalescence is lower because of the high viscosity of the PB phase; therefore, PB becomes a continuous matrix. An interpenetrating cocontinuous morphology is obtained for the 50/50 PS/PB system, as seen in Figure 1(d). At this particular composition, both immiscible phases are

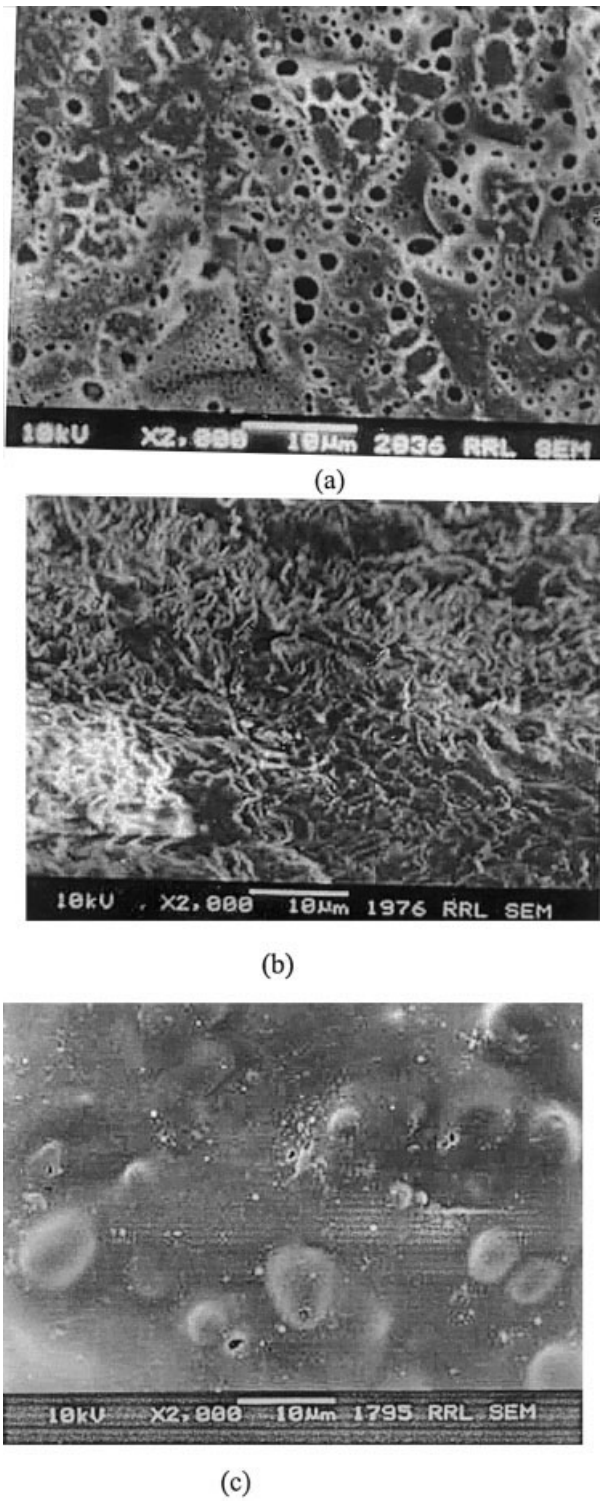

Figure 3 SEM micrographs of binary PS/PB blends after dissolution experiments: (a) 30/70, (b) 50/50, and (c) 70/30.

completely continuous (100% continuous), and there is no possible distinction between the matrix and the dispersed phase. This is followed by a phase inversion. In S_{60} in Figure 1(e), both dispersed and continuous phases are seen. However, for S_{70}, the minor phase of PB is dispersed as droplets in the continuous PS matrix, as seen in Figure 1(f). Therefore, Figure 1(f,g) gives a dispersed morphology in which PB is dispersed in the continuous PS matrix. The effect of the blend composition on the dispersed particle size is shown in Figure 2. The continuity of the phases, as shown in Figure 1(d), complements the aforementioned observations. As expected, most blends show an increase in the average particle diameter as the amount of the dispersed phase increases. This is typically related to droplet coalescence during melt mixing, which is known to be a random process, broadening the particle size distribution. The dispersed PB blends have larger domain diameters than their counterparts of dispersed PS domains. There are several reports on this observed phenomenon.[19–22] Therefore, an asymmetric influence of phase coarsening is observed in the same blend system. This can be explained as, according to the viscosity ratio of the components, the amount of coalescence differs. Because the interfacial tension in all blends is nearly the same, it is the viscosity ratio that affects the droplet breakup and coalescence rate. The morphology of samples S_{30}, S_{50}, and S_{70} after dissolution experiments was also studied by SEM [Fig. 3(a–c)]. Morphological observations similar to those in Figure 1 are also seen here. The various domain diameters calculated according to eqs. (1)–(4) from micrographs of etched samples are given in Table II. Blends of dispersed PB and PS phases show differences in their domain diameters. This asymmetric behavior can be explained by the lower melt viscosity of the PS phase in comparison with that of the PB matrix phase. As a result, the equilibrium between breakup and coalescence is shifted more in the direction of coalescence in PS-rich blends.

The melt viscosity of pure polymers at 180°C, as measured with capillary rheometry, is given in Figure 4. PB has a higher melt viscosity than PS. It In many rubber/plastic blends, the rubbers often exhibit higher melt viscosity than the plastics. The viscosity ratios of the blend components are obtained by the division of the viscosity functions of the dispersed phase and the matrix polymer. To better analyze the shear rate influence on the rheology and morphology, we calculated the viscosity ratios of the two systems at various shear rates, as given in Table III. The viscosity ratios are greater than 1 when PB is dispersed in the continuous PS matrix and are considerably less than 1 when PS is

TABLE II
Various Domain Diameters Calculated According to Eqs. (1)–(4)

Blends	$\bar{D}_n$ (μm)	$\bar{D}_w$ (μm)	$\bar{D}_s$ (μm)	$\bar{D}_v$ (μm)	PDI
S_{70} (ext)	4.52	4.86	4.64	10.02	1.02
S_{30} (ext)	3.60	4.62	3.95	5.01	1.28

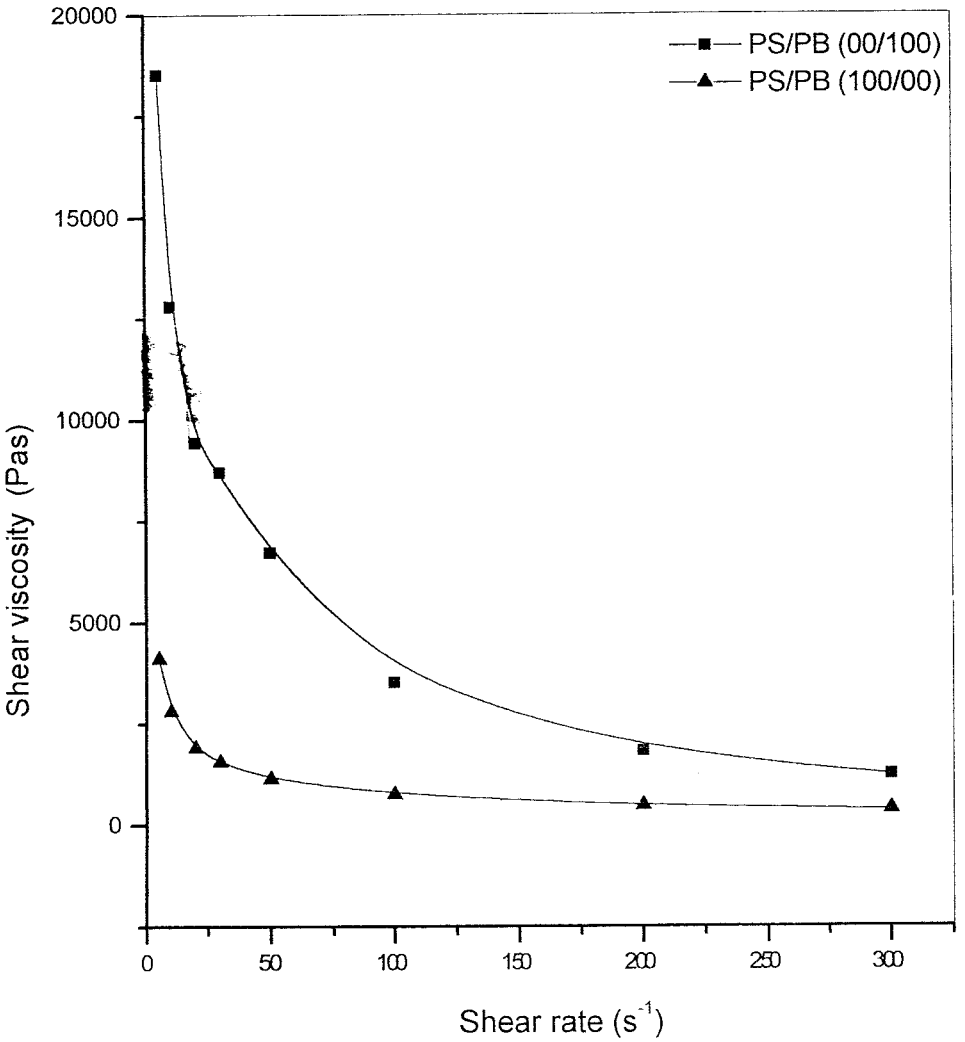

Figure 4 Melt viscosities of the homopolymers at 180°C and at different shear rates.

the dispersed phase at all shear rates analyzed. A significant deformation of the dispersed phase along the flow direction can then be expected.[25] When the viscosity ratio is above unity, the dispersed particle becomes larger. The smallest particles are obtained when the viscosity ratio is 1, other factors being equal. However, viscoelastic drops can break up during extrusion even when the viscosity ratio is greater than 4 because of elastic effects, the presence of an elongational field, and the complex viscosity/temperature profile along the extruder barrel. This is different from the case of a Newtonian drop in a Newtonian matrix in uniform steady shear.

TABLE III
Viscosity (η) and Viscosity Ratio of the Blend Components of PS and PB

Shear rate (s^{-1})	η_{PB}	η_{PS}	η_{PB}/η_{PS}	η_{PS}/η_{PB}
5	18527	4119	4.45	0.22
10	12806	2814.	4.93	0.20
20	9443	1916	5.90	0.17
30	8713	1563.	4.66	0.21
50	6725.	1140	3.78	0.26
100	3527	756	3.27	0.31
200	1835	486	3.78	0.26
300	1242	380	3.26	0.31

The method of macroscopic characterization by solvent dissolution testing is summarized in Table IV. The results are in good agreement with the morphology obtained from SEM observations. This test gives results in a shorter time for macroscopic characterization so that it can be carried out in all blend samples. The PS-poor blends S_{10}, S_{20}, and S_{30} are disintegrated in butan-2-one, whereas S_{40}, S_{50}, and S_{60} do not disintegrate, showing an onset of percolation and cocontinuity. From samples having PS contents greater than 50 and etched in butan-2-one, a jelly mass is obtained. Similarly, the PB-poor blends S_{70} and S_{80} are disintegrated in *n*-heptane, whereas other blends show no disintegration in the solvent.

TABLE IV
Results of Disintegration Tests of the Different Blend Series

Sample code	Dissolution etchant: Butan-2-one for PS phase	Dissolution etchant: *n*-Heptane for PB phase
S_{10}	D	ND
S_{20}	D	ND
S_{30}	D	ND
S_{40}	PD	ND
S_{50}	ND	ND
S_{60}	ND	PD
S_{70}	ND	D
S_{80}	ND	D

D = disintegration; ND = no disintegration; PD = partial disintegration.

It is also possible to estimate the continuity of the phases from these tests. The results of disintegration tests of the different blend series show the effectiveness of dissolution (Table V). At 10% PS, the level of continuity is nearly zero, which confirms the morphological observation of dispersed droplets at concentrations less than S_{20}. At 20% PS, continuity increases considerably to a volume fraction of 0.15. At S_{30}, continuity still increases to around 0.45. The results confirm the morphological study that placed the percolation threshold for dispersed PS between S_{10} and S_{20}. Between S_{40} and S_{50} and S_{50} and S_{60}, a semicontinuous morphology is observed. At S_{50}, there is phase inversion, and beyond this, PB is seen to be dispersed in the PS phase. Between S_{60} and S_{80}, continuity increases gradually and reaches a volume fraction 0.98 at S_{80}. A similar trend is observed when *n*-heptane is used as an etchant for the PB phase. The experimentally observed region of dual-phase continuity is seen at a volume fraction of PS equal to 0.43 and at a volume fraction of PB equal to 0.57. In terms of the weight percentage, the region of cophase continuity is at 50/50 PS/PB.

The prediction of phase inversion has been conducted with the different models mentioned previously. The values of $\eta_1\phi_2/\eta_2\phi_1$ at different shear rates according to the Jordhamo model are given in Table VI. According to this model, the observed region of dual-phase continuity is predicted at very low shear rates, (5, 10, and 20 s^{-1}). Therefore, we come to the conclusion that a phase-inversion composition is observed in a high PB composition range at low shear rates. This model, however, is limited to low shear rates and does not consider the variations in the interfacial tension between the phases. This equation does not always predict the region of phase inversion correctly, especially for the blending of materials with large differences in the melt viscosities.

The volume fractions at the point of phase inversion, obtained for PS and PB, by the application of these models are quantified in Table VII. The data obtained by the application of all the models described by eqs. (8)–(11) suggest that the less viscous phase will have the greatest tendency to become a continuous phase. Therefore, the blending of a highly viscous material and a low viscous material causes the region of cocontinuity to shift toward the low viscous phase. Similar reports were already made by Everaert et al.[17] and Favis and Chalifoux.[21,22] The observed point of phase inversion, as suggested by these models, is not in agreement with that of morphological and dissolution tests. The wide disparity observed for the point of phase inversion, as obtained from morphological and dissolution studies, when compared with these models, leads us to the conclusion that these models need some modification. The only aspects treated in these models are the viscosity and volume ratio, which alone are not sufficient for predicting the location of phase inversion. Other parameters such as the absolute viscosity, rather than the viscosity ratio, the phase dimensions, the mixing conditions, and the interfacial tensions also need to be taken into account in determining the location of the point of phase inversion

CONCLUSIONS

The phase inversion in a PS/PB blend system was investigated with different techniques. A disintegration test in a selective solvent for one of the blend components was found to be a very suitable technique for identifying the type of phase morphology; whether it

TABLE V
Volume Fraction of the Different Blend Series After the Disintegration Tests

Sample code	Cocontinuity index of PS	Cocontinuity index of PB
S_{10}	0.09	0.92
S_{20}	0.15	0.81
S_{30}	0.45	0.80
S_{40}	0.62	0.79
S_{50}	0.95	0.70
S_{60}	0.97	0.37
S_{70}	0.97	0.17
S_{80}	0.98	0.06

TABLE VI
Values of $\eta_1\phi_2/\eta_2\phi_1$ at Different Shear Rates According to the Jordhamo model [Eq. (7)]

Shear rate (s^{-1})	S_{20}	S_{30}	S_{40}	S_{50}	S_{60}	S_{70}	S_{80}
5	1.01	1.74	2.71	4.06	6.09	9.48	16.26
10	1.02	1.76	2.74	4.11	6.17	9.59	16.45
20	1.11	1.90	2.97	4.45	6.68	10.39	17.82
30	1.25	2.15	3.35	5.03	7.55	11.75	20.15
50	1.33	2.28	3.55	5.33	7.99	12.44	21.33
100	1.05	1.80	2.81	4.21	6.32	9.83	16.87
200	0.85	1.46	2.27	3.41	5.11	7.96	13.65
300	0.73	1.26	1.96	2.95	4.43	6.89	11.81

TABLE VII
Prediction of the Phase-Inversion Point as a Function of Viscosity Ratio

Shear rate (s^{-1})	Jordhamo model		Paul and Barlow model		Chen and Su model		Modified Chen and Su model		Metlkin and Blekht model	
	ϕ PS	ϕ PB	ϕ PS	ϕ PB	ϕ PS	ϕ PB	ϕ PS	ϕ PB	ϕ PS	ϕ PB
5	0.18	0.82	0.81	0.18	0.93	0.06	0.84	0.15	0.93	0.06
10	0.16	0.84	0.81	0.18	0.93	0.06	0.84	0.15	0.93	0.06
20	0.14	0.86	0.83	0.16	0.94	0.05	0.85	0.14	0.94	0.05
30	0.21	0.79	0.84	0.15	0.95	0.04	0.86	0.13	0.95	0.04
50	0.31	0.69	0.85	0.14	0.95	0.04	0.87	0.12	0.95	0.04
100	0.23	0.77	0.82	0.17	0.93	0.06	0.84	0.15	0.93	0.06
200	0.20	0.80	0.79	0.20	0.92	0.07	0.81	0.18	0.91	0.08
300	0.23	0.77	0.76	0.23	0.89	0.10	0.79	0.20	0.89	0.10

ϕ = volume fraction. Experimental $\phi PS^{\#} = 0.47$ and $\phi PB = 0.53$. $\phi PS^{\#}$ refers to the PS volume fraction at the point of phase inversion.

was matrix droplet or cocontinuous. SEM was used to investigate the phase morphologies as a function of the blend ratio. In all the morphological analyses, PS was the dispersed phase up to S_{30}. Between S_{40} and S_{50} and S_{50} and S_{60}, a cocontinuous morphology was observed. In S_{50}, cophase continuity was visible. Beyond S_{50}, phase inversion occurred, and PB became the dispersed phase. There was good agreement between the results of the disintegration tests and the morphology analysis by SEM for determining the phase inversion and cocontinuity. Various theoretical models were applied to quantify the volume fractions at the point of phase inversion. The point of phase inversion suggested by these models was not in close agreement with experimental observations in morphology and dissolution tests. In addition to viscosity ratios, other parameters such as the melt elasticity, interfacial tension, absolute viscosity (rather than viscosity ratio), phase dimensions, and mixing conditions were found to influence cocontinuity decisively. Therefore, an adequate consideration of these factors should also be made during a study of cocontinuity. The wide disparity observed for the point of phase inversion, as obtained from morphological and dissolution studies, when compared with these models, has led us to the conclusion that these models need some modification, and a comprehensive model incorporating elastic, viscous, and morphological effects is to be developed.

References

1. Walker, B. M. Handbook of Thermoplastic Elastomers; Van Nostrand Reinhold: New York, 1979.
2. Wu, S. Polymer 1985, 26, 1855.
3. Shin, B.; Jang, Y.; Chung, S. H.; Kim, B. S. Polym Eng Sci 1992, 32, 73.
4. Machiels, A. G. C.; Denys, K. F. J.; Van Dam, J.; De Boer, A. P. Polym Eng Sci 1997, 37, 59.
5. Verhoogt, H.; Willemse, R. C.; Van Dam, J.; De Boer, A. P. Polym Eng Sci 1994, 34, 453.
6. Submaranian, P. M. Polym Eng Sci 1987, 27, 663.
7. Willemse, R. C.; Speijer, A.; Langeraar, A. E.; De Boer, A. P. Polymer 1999, 40, 6645.
8. Metelkin, V. I.; Blekht, V. S. Colloid J USSR 1984, 46, 425.
9. Arns, C. H.; Knackstedt, M. A.; Roberts, A. P.; Pinczewski, V. W. Macromolecules 1999, 32, 5964.
10. Lee, J. K.; Han, C. D. Polymer 1999, 40, 2521.
11. Veenstra, H.; Barbara van Lent, B. J. J.; Van Dam, J.; Posthuma de Boer, A. Polymer 1999, 40, 6661.
12. Gorton, D. T.; Pendle, T. D. NR Technol 1981, 12, 1.
13. Bourry, D.; Favis, B. D. J Polym Sci Part B: Polym Phys 1996, 36, 1891.
14. Bu, W.; He, J. J Appl Polym Sci 1996, 62, 1445–1456.
15. Jordhamo, G. M.; Manson, J. A.; Sperling, L. H. Polym Eng Sci 1986, 26, 517.
16. Chen, T. H.; Su, A. C. Polymer 1993, 34, 4826.
17. Everaert, V.; Aerts, L.; Groeninckx, G. Polymer 1999, 40, 6627.
18. Paul, D. R.; Barlow, J. W. J Macromol Sci Rev Macromol Chem 1980, 18, 109.
19. Avgeropoulos, C. N.; Weissert, F. C.; Biddison, P. H.; Bhom, G. G. A. Rubber Chem Technol 1979, 49, 93.
20. Jorgensen, L.; Utracki, L. A. Makromol Chem Macromol Symp 1991, 48, 189.
21. Favis, B. D.; Chalifoux, J. P. Polymer 1988, 29, 1761.
22. Favis, B. D.; Chalifoux, J. P. Polym Eng Sci 1987, 27, 1591.
23. Utracki, L. A. J Rheol 1991, 35, 1615.
24. Van Oene, H. Colloid J USSR 1984, 46, 425.
25. Han, D. H. Multiphase Flow in Polymer Processing; Academic: New York, 1981.